

Phase diagram and influence of defects in the double perovskites

J. L. Alonso,^{1,2} L. A. Fernández,^{3,2} F. Guinea,^{4,2} F. Lesmes,⁵ and V. Martín-Mayor^{3,6}

¹Departamento de Física Teórica, Facultad de Ciencias,
Universidad de Zaragoza, 50009 Zaragoza, Spain.

²Instituto de Biocomputación y Física de Sistemas Complejos (BIFI). Universidad de Zaragoza, 50009 Zaragoza, Spain.

³Departamento de Física Teórica, Facultad de Ciencias Físicas,
Universidad Complutense de Madrid, 28040 Madrid, Spain.

⁴Instituto de Ciencia de Materiales (CSIC). Cantoblanco, 28049 Madrid. Spain.

⁵Centro de Astrobiología. INTA-CSIC. Carretera de Ajalvir km 4, 28850 Torrejón de Ardoz, Madrid, Spain.

⁶Dipartimento di Fisica, Università di Roma "La Sapienza", INFN,
SMC and UdR1 of INFM, P.le Aldo Moro 2, 00185 Roma, Italy.

(Dated: 14th October 2002)

The phase diagram of the double perovskites of the type $\text{Sr}_{2-x}\text{La}_x\text{FeMoO}_6$ is analyzed, with and without disorder due to antisites. In addition to an homogeneous half metallic ferrimagnetic phase in the absence of doping and disorder, we find antiferromagnetic phases at large dopings, and other ferrimagnetic phases with lower saturation magnetization, in the presence of disorder.

PACS numbers: 75.30.Vn, 75.10.-b.

Introduction. The double perovskite $\text{Sr}_2\text{FeMoO}_6$ and related materials¹ are good candidates for magnetic devices, as they combine a high Curie temperature and a fully polarized (half metallic) conduction band.² At present, these materials are being extensively studied.^{3,4,5,6,7,8,9,10,11,12,13,14,15}

The magnetism of these compounds arises from the Fe^{3+} , $S = 5/2$ core spin, while the charge state of the Mo ion is 5+. Spatially, the Mo and Fe ions occupy two interleaving FCC lattices (sodium chloride structure). The conduction band contains one electron per unit cell, which tends to be antiparallel to the Fe spin. Experiments suggest that, in many samples, the saturation magnetization is less than the expected $4\mu_B$ per formula unit. This effect is usually ascribed to the presence of antisite defects,^{3,5,8,9,10,11,13,14,16,17} where, due to the similarity of their atomic radii, Mo ions are randomly placed on the Fe sublattice and conversely. Notice that when a Fe ion is misplaced, with high probability it will have a Fe ion among its first neighbors, enhancing direct antiferromagnetic (AFM) superexchange with respect to the ideal structure. The strength of this coupling can be inferred from the compound LaFeO_3 , which has the same structure, but where the Mo ions have been substituted by Fe^{3+} . LaFeO_3 is known to be AFM,¹⁸ with a Néel temperature of $T_N = 720\text{K}$.

The Sr ions in $\text{Sr}_2\text{FeMoO}_6$ can be substituted for triva-

lent cations, like La, leading to $\text{Sr}_{2-x}\text{La}_x\text{FeMoO}_6$.^{4,8,13} These compounds have $1+x$ electrons per formula unit in the conduction band. These doped materials tend to have a higher Curie temperature. Notice that one can also consider the substitution with a monovalent ion (*i.e.* $\text{Sr} \rightarrow \text{K}$, $\text{Sr}_{2-x}\text{K}_x\text{FeMoO}_6$), which takes one electron from the conduction band, leaving $1-x$ electrons per formula unit. Hence in this paper negative x will actually refer to substitution with a monovalent ion.

The model. Band structure calculations have shown that the conduction band can be described in terms of hybridized t_{2g} orbitals at the Mo and Fe sites.^{2,19} If one considers the t_{2g} orbitals of both spin orientations at the Fe sites, the model leads to a highly correlated system, where an on site Hund's coupling and a Hubbard repulsive term have to be added.^{20,21,22} In the following, we will consider the magnetic phase diagram only, and neglect the possible existence of a metal-insulator transition when the ratio between the bandwidth and the Coulomb term is sufficiently small.^{21,22} We consider that the conduction band is built up of the three t_{2g} orbitals at the Fe sites with spins oriented antiparallelly to the Fe moment, and the six t_{2g} orbitals at the Mo sites (see below).

We denote the destruction operator on xy orbitals with spin + or - at lattice site \mathbf{r} as $F_{xy;\pm;\mathbf{r}}$, $M_{xy;\pm;\mathbf{r}}$ (F for Fe and M for Mo), and so on. The spin and number operators on a given Fe site are:

$$\vec{S}_{\mathbf{r}} = \sum_{\alpha, \beta = \pm} (F_{xy;\alpha;\mathbf{r}}^\dagger + F_{xz;\alpha;\mathbf{r}}^\dagger + F_{yz;\alpha;\mathbf{r}}^\dagger) \vec{\sigma}_{\alpha, \beta} (F_{xy;\beta;\mathbf{r}} + F_{xz;\beta;\mathbf{r}} + F_{yz;\beta;\mathbf{r}}) , \quad (1)$$

$$\mathcal{N}_{\mathbf{r}}^{\text{Fe}} = \sum_{\alpha = \pm} (F_{xy;\alpha;\mathbf{r}}^\dagger F_{xy;\alpha;\mathbf{r}} + F_{xz;\alpha;\mathbf{r}}^\dagger F_{xz;\alpha;\mathbf{r}} + F_{yz;\alpha;\mathbf{r}}^\dagger F_{yz;\alpha;\mathbf{r}}) . \quad (2)$$

Analogous definitions hold for the Mo atoms. Given the

large spin value ($S=5/2$) of the the localized Fe core spins,

we treat them as classical, with polar coordinates

$$\vec{\phi} = (\sin \theta \cos \varphi, \sin \theta \sin \varphi, \cos \theta) \quad (3)$$

As mentioned above, we only consider the Fe orbitals with spin antiparallel to $\vec{\phi}$, which amounts to assume that the Hund's coupling at the Fe ions is much larger than the other interactions. Thus, we define up and down orbitals, f_1 and f_2 , with respect to the local $5/2$ spin:

$$\begin{aligned} F_+ &= \cos \frac{\theta}{2} f_1 + \sin \frac{\theta}{2} f_2, \\ F_- &= \sin \frac{\theta}{2} e^{i\varphi} f_1 - \cos \frac{\theta}{2} e^{i\varphi} f_2, \end{aligned} \quad (4)$$

and we neglect all terms including the f_1 operators. For the sake of brevity, in the following we set $f_2 = f$. Then, the Hamiltonian, in the absence of disorder and neglecting direct hopping terms between Mo orbitals (see below), can be written as:

$$\mathcal{H} = \mathcal{K}_{xy} + \mathcal{K}_{yz} + \mathcal{K}_{xz} - \mu \sum_{\mathbf{r}_{\text{even}}} \mathcal{N}_{\mathbf{r}}^{\text{Fe}} - (\mu + \Delta) \sum_{\mathbf{r}_{\text{odd}}} \mathcal{N}_{\mathbf{r}}^{\text{Mo}}, \quad (5)$$

with

$$\mathcal{K}_{xy} = t_{\text{Mo-Fe}} \sum_{\substack{\mathbf{r} \in \text{Fe lattice} \\ \hat{u} = \hat{e}_x, \hat{e}_y}} (\sin \frac{\theta_{\mathbf{r}}}{2} f_{xy; \mathbf{r}}^\dagger M_{xy; +; \mathbf{r} + \hat{u}} + \text{h.c.}) \dots \quad (6)$$

where, for brevity, we omit the analogous hoppings from the sites belonging to the Mo sublattice to the Fe sites. Analogous expressions are found for the kinetic energy on the xz and yz planes. Finally, we add a direct hopping between Mo orbitals. These hopping terms give rise to three separate two dimensional Hamiltonians.^{20,21,22} The substitution of Mo ions for Fe ions leads to direct Fe-Fe hopping terms, (we take $t_{\text{Fe-Fe}} = t_{\text{Mo-Fe}}$), and also to the inclusion of an AFM exchange, $J_{\text{Fe-Fe}}$. Thus, the model is defined by the parameters $t_{\text{Mo-Fe}}$, $t_{\text{Mo-Mo}}$, Δ , μ and $J_{\text{Fe-Fe}}$. There are nine orbitals per unit cell, three at the Fe sites, and six at the Mo sites.

The occupancy of the conduction band depends on the value of the chemical potential, μ , and it varies from one electron to two electrons per unit cell in $\text{Sr}_{2-x}\text{La}_x\text{FeMoO}_6$, $0 \leq x \leq 1$. We neglect interactions of the electrons within this band (as discussed below, the number of electrons at the Fe sites is always less than one).

We will use $t_{\text{Fe-Mo}}$ as our unit of energy ($t_{\text{Fe-Mo}} \approx 0.35\text{eV}$ from band structure calculations). We take $t_{\text{Mo-Mo}}/t_{\text{Fe-Mo}} = 0.25$, $\Delta = 0$ and $J_{\text{Fe-Fe}}/t_{\text{Fe-Mo}} = 0.1$. The value of Δ implies a relatively large hybridization of the Fe and Mo orbitals, which seems consistent with Hartree-Fock calculations.²² $J_{\text{Fe-Fe}}$ is chosen so as to reproduce the Néel temperature of LaFeO_3 . We have not made a comprehensive study of the dependence of the results on the tight binding parameters, but the calculations made so far indicate that the qualitative features of

the phase diagrams to be discussed below are not strongly dependent on the choice of parameters. In the absence of disorder, this model is basically equivalent to the one studied by Chattopadhyay and Millis²⁰ in the context of Dynamical Mean Field Theory, although we shall use Variational Mean Field (see 23 for a comparison between the two methods). The main novelty is in our considering of the disorder effects^{3,5,8,9,10,11,13,14,17}: with probability y we misplace an Fe ion onto the Mo sublattice (and conversely) without any spatial correlations (y is just the antisite density). It is clear that $y = 0.5$ corresponds to full disorder on the location of the Fe and Mo ions, while $y > 0.5$ is equivalent to $1 - y$ with the Fe and Mo sublattices interchanged. Vacancies can be equally considered, but explicit calculations showed that they have a much milder effect on the phase diagram.

Method of calculation. We use the method developed for double exchange systems in Ref. 23. We assume that the Fe core spins are classical. At a given temperature, we average over spin configurations obtained by assuming that there is a magnetic field acting on the spins. The magnitude of these fields are variational parameters, which are taken so as to minimize the free energy. Given a spin configuration, the electronic states are calculated exactly, and the electronic contribution to the free energy is obtained by integrating the density of states. As the Fe spins are distributed in a three dimensional lattice, and the electrons lead to effective interactions with the cubic symmetry, we think that our mean field ansatz for the spin configurations is sufficient. This method is in excellent agreement with more precise Monte Carlo calculations for the double exchange model.²⁴ We solve the Hamiltonian in lattices with up to $512 \times 512 \times 512$ sites (note that the calculation of the electronic wave functions requires only the diagonalization of the Hamiltonian in a 512×512 square). For these sizes, the disorder due to antisites is self-averaging.

The adequacy of our technique depends on the ansätze made for the possible spin configurations. We have considered four possible phases: i) the paramagnetic (PM) phase, ii) the ferrimagnetic (FI) phase, where all Fe spins are parallel, and the spins of the electrons in the conduction band are antiparallel to the Fe spins, iii) an AFM phase, where the Fe spins in neighboring (1,1,1) planes are antiparallel, and iv) a different ferrimagnetic (FIP) phase where the Fe spins are aligned ferromagnetically if the Fe are in the correct positions, and antiferromagnetically if the Fe ions occupy Mo sites because of the antisite defects. In the absence of disorder, we have checked that other phases with canted spins have higher free energy. Note that the above ansätze define the average magnetization at the Fe sites, but that thermal fluctuations are also included.

Results. The phase diagram of $\text{Sr}_{2-x}\text{La}_x\text{FeMoO}_6$, as function of x and temperature, is shown in Fig. 1 for different concentrations of antisites.

In the absence of defects, we find that T_C decreases with increasing doping of the conduction band, in agree-

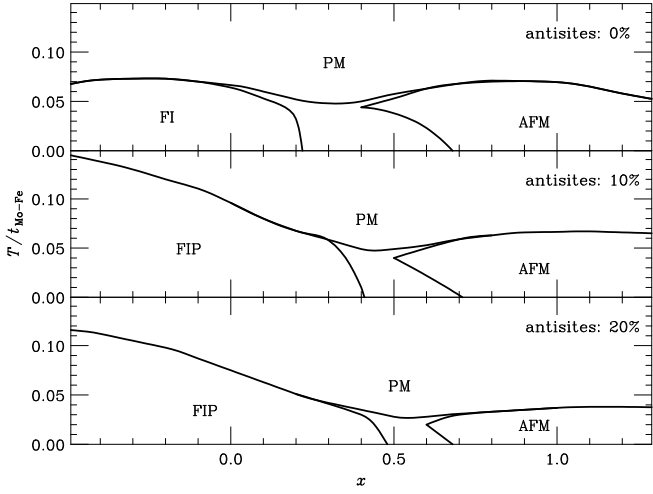


Figure 1: Phase diagram of $\text{Sr}_{2-x}\text{La}_x\text{FeMoO}_6$ as function of x and temperature for different concentrations of antisite defects. Negative x actually means $\text{Sr}_{2-|x|}\text{K}_{|x|}\text{FeMoO}_6$. In both cases, the density of carriers in the conduction band is $1+x$. Phase-separation regions are found between the FI and AFM phases (upper panel), and between the FIP and AFM phases (middle and lower panel).

ment with Ref. 20. At high, but still reasonable, dopings we find the ordered AFM phase described above. The phase transitions are first order, with regions of phase separation between them. For $x \approx 0$, the spins of the electrons at the Mo orbitals are antiparallel to the Fe core spins. We ascribe the tendency toward phases with zero magnetization, upon increasing doping, to the occupancy of the Mo orbitals which are aligned parallel to the Fe spins.

The presence of antisite defects changes significantly the phase diagram: i) The FI phase is replaced by the FIP phase, where the spins at the Fe sites at the defects are antiparallel to the overall magnetization, ii) the ordered AFM phase is strongly suppressed, and iii) the value of T_C increases as the concentration of antisites also increases²⁶, iv) the dependence of T_C with the number of electrons in the conduction band is more pronounced in the presence of antisites.

These effects are associated to the direct AFM interaction between spins at Fe ions which are nearest neighbors. These interactions play no role in perfect materials. The antiferromagnetic interaction can be easily shown to be equivalent to a *ferromagnetic* one for the atoms in the Fe sublattice. Thus, superexchange enhances the tendency toward a ferromagnetic order in the original Fe sublattice. This effect is independent of the number of electrons in the conduction band. The saturation magnetization, on the other hand, is reduced.

Fig. 2 gives the occupancies of the different orbitals as the number of electrons in the conduction band is varied. Most of the charge is in the Mo orbitals. The variation is not linear, indicating that a rigid band picture is not valid.¹⁷ There are sharp changes at the phase transitions.

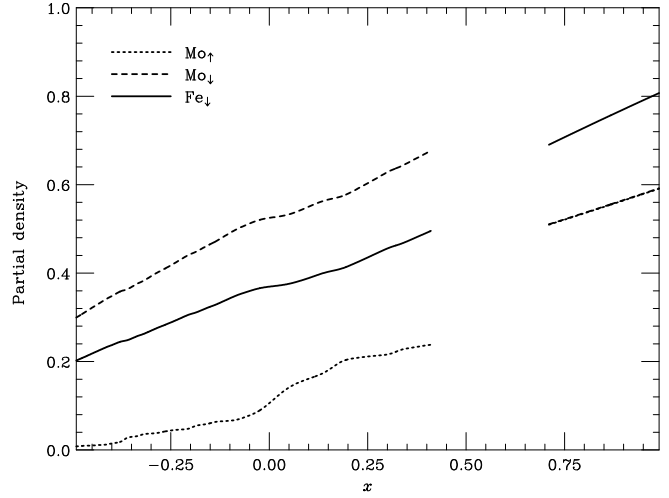


Figure 2: Occupation of the Mo_\uparrow , Mo_\downarrow and Fe_\downarrow as function of the doping of the conduction band. The curves give the occupancies for a 10% density of antisites defects. Note that in phases with no net magnetization, the occupancies of the Mo_\uparrow and Mo_\downarrow levels are the same.

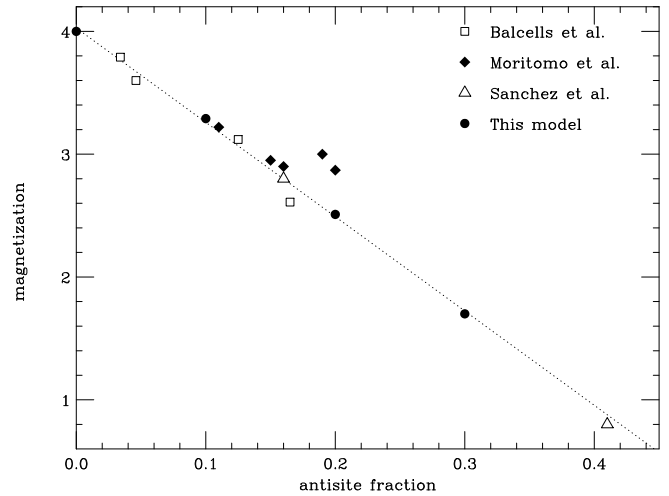


Figure 3: Low temperature magnetization (μ_B per formula unit) of $\text{Sr}_2\text{FeMoO}_6$ as function of the concentration of antisite defects, y . Experimental results are from Refs. 9,11,14.

At low temperatures, the spins at antisites tend to be antiparallel to the magnetization, as shown in Fig. 1. This implies that the saturation magnetization is reduced with respect to the ordered case. The total magnetization of the core spins and the conduction electrons, is shown in Fig. 3. The calculated magnetization is well fitted by the line $M_S = (4.0 - 7.7y)\mu_B$, where y is the antisite density. Experimental results from Refs. 9,11,14. are added for comparison. Note that the decrease in the magnetization does not lead to a lowering of the Curie temperature, as discussed above.

Conclusions. We have studied the magnetic phase diagram of the doped double perovskites, $\text{Sr}_{2-x}\text{La}_x\text{FeMoO}_6$.

We have analyzed the influence of antisite defects, on the phase diagram.

In clean systems, we find that, as the number of electrons in the conduction band increases, the critical temperature decreases, in agreement with previous calculations.²⁰ This variation is due to the increased filling of the Mo_{\uparrow} band, which reduces the double exchange-like mechanism which tends to align the Fe moments. At sufficiently high dopings, we find ordered phases without net magnetization, which enhance the delocalization of both the Mo_{\uparrow} and Mo_{\downarrow} bands. The transitions between these phases tend to be first order, with regions of phase separation between them. Electrostatic effects will prevent the existence of phase separation at macroscopic scales, leading to a domain structure at mesoscopic scales²⁵.

Antisite disorder induces significant changes in the phase diagram. The ordered ferrimagnetic phase is replaced by a different ferrimagnetic phase where the Fe spins at defects are antiparallel to the bulk magnetization (the FIP phase, see Fig.1). Antiferromagnetism at finite dopings is suppressed. The saturation magnetization in the FIP phase is reduced, although the Curie temperature tends to increase with the number of Fe in Mo positions, due to the direct AFM exchange between Fe ions which are nearest neighbors²⁶.

Note that, in order to study compounds with different number of carriers in the conduction band, the presence of vacancies and changes in the Fe - O - Mo bond angles,

Fe/Mo - O distance, and in the energy splitting Δ can influence the results. These effects need to be extracted from the available experimental data and incorporated in the model Hamiltonian, eq. (5).

We have not studied transport properties, although it seems likely that the variation of the magnetic structure near defects will lead to significant changes in a half metallic system.¹⁷ We have also not analyzed other effects of the electron-electron interaction, such as the existence of a Mott transition to an insulating state, found in the related compound Sr_2FeWO_6 .²² We think, however, that our model includes all relevant interactions required to study the magnetic properties of the metallic state of double perovskites. Similar models provide a good understanding of the magnetic properties of the half metallic manganite oxides (such as $\text{La}_{1-x}\text{Ca}_x\text{MnO}_3$).^{23,24}

In summary, we find a rich phase diagram for $\text{Sr}_{2-x}\text{La}_x\text{FeMoO}_6$, which is significantly modified in the presence of defects. Our results seem consistent with existing experimental data.

Acknowledgements. We are thankful to J. Blasco, M. Coey, J. Fontcuberta, M. García-Hernández, R. Ibarra, J. L. Martínez, L. Morellón, D. D. Sarma, and D. Serrate, M. Venkatesan, and especially to V. Laliena, for helpful discussions. VMM was supported by E.C. contract HPMF-CT-2000-00450 and by a *Ramon y Cajal* contract (Spain). Financial support from grants PB96-0875, FPA2000-0956, FPA2000-1252, FPA2001-1813 (MCyT, Spain), and 07N/0045/98 (C. Madrid) are acknowledged.

¹ A. W. Sleight and J. F. Weiher, *J. Phys. Chem. Solids* **33**, 679 (1972).

² K. I. Kobayashi, *et al.*, *Nature* **395**, 677 (1998); *Phys. Rev. B* **59**, 11159 (1999).

³ A. S. Ogale, *et al.*, *Appl. Phys. Lett.* **75**, 537 (1999).

⁴ Y. Moritomo, *et al.*, *Phys. Rev. B* **62**, 14224 (2000).

⁵ D. D. Sarma, *et al.*, *Solid State Commun.* **114**, 465 (2000).

⁶ J. Gopalakrishnan, *et al.*, *Phys. Rev. B* **62**, 9538 (2000).

⁷ C. Ritter, *et al.*, *J. Phys.: Condens. Matter* **12**, 8295 (2000).

⁸ J. Navarro, *et al.*, *Phys. Rev. B* **64**, 092411 (2001).

⁹ Ll. Balcells, *et al.*, *Appl. Phys. Lett.* **78**, 781 (2001).

¹⁰ M. García-Hernández, *et al.*, *Phys. Rev. Lett.* **86**, 2443 (2001).

¹¹ Y. Moritomo, *et al.*, *Jpn. J. Appl. Phys.* **40**, L672 (2001).

¹² J. M. Greneche, *et al.*, *Phys. Rev. B* **63**, 174403 (2001).

¹³ D. Serrate, *et al.*, *Appl. Phys. Lett.* **80**, 4573 (2002).

¹⁴ D. Sánchez, *et al.*, *Phys. Rev. B* **65**, 104426 (2002).

¹⁵ M. Tovar, *et al.*, *Phys. Rev. B* **66**, 024409 (2002).

¹⁶ M. Venkatesan, *et al.*, *Journ. Magn. and Mag. Mat.* **242-245**, 744 (2002).

¹⁷ T. Saha-Dasgupta and D. D. Sarma *Phys. Rev. B* **64**, 064408 (2001).

¹⁸ T. M. Rearick, G. L. Catchen and J. M. Adams, *Phys. Rev. B* **48**, 224 (1993).

¹⁹ D. D. Sarma, *et al.*, *Phys. Rev. Lett.* **85**, 2549 (2000).

²⁰ A. Chattopadhyay and A. J. Millis, preprint cond-mat/0006208, *Phys. Rev. B* **64**, 024424 (2001).

²¹ A. A. Aligia, P. Petrone, J. O. Sofo, and B. Alascio, *Phys. Rev. B* **64**, 092414 (2001).

²² P. Petrone and A. A. Aligia, preprint cond-mat/0207325.

²³ J. L. Alonso, *et al.*, *Phys. Rev. B* **63**, 54411 (2001); *ibid* **63**, 064416 (2001).

²⁴ J. L. Alonso, *et al.*, *Nucl. Phys. B* **596**, 587 (2001); J. L. Alonso, *et al.*, *Phys. Rev. B* **64**, 054408 (2001).

²⁵ F. Guinea, G. Gómez-Santos, and D. P. Arovas, *Phys. Rev. B* **62**, 391 (2000).

²⁶ Our estimate of $J_{\text{Fe-Fe}}/t_{\text{Fe-Mo}} = 0.1$ gives a lower bound to this anomalous dependence of T_C on the number of defects. A lower, but physically reasonable, value for $t_{\text{Fe-Mo}}$ than the one used here, $t_{\text{Fe-Mo}} \approx 0.35\text{eV}$, leads to a more pronounced increase of T_C as function of the number of antisite defects, for fixed doping.